

Multiple-chain phase separation and single-chain compactness of charged disordered proteins are strongly correlated

Yi-Hsuan Lin^{1,2} and Hue Sun Chan^{1,3}

¹Department of Biochemistry, University of Toronto, 1 King's College Circle, Toronto, Ontario M5S 1A8, Canada; ²Molecular Structure and Function Program, Hospital for Sick Children, 686 Bay Street, Toronto, ON M5G 0A4, Canada; ³Department of Molecular Genetics, University of Toronto, Toronto, 1 King's College Circle, Ontario M5S 1A8, Canada

ABSTRACT A recent formulation of random-phase-approximation polymer theory for disordered protein phase separation is applied to investigate how the tendency for multiple chains of a protein to phase separate, as characterized by the critical temperature T_{cr}^* , is related to the protein's single-chain average radius of gyration $\langle R_g \rangle$. For a set of thirty model sequences containing different permutations of an equal number of positively and negatively charged residues, we found a striking correlation $T_{cr}^* \sim \langle R_g \rangle^{-\nu}$ with $\nu \approx 3.5\text{--}6.0$, indicating that electrostatic effects have similar impact in promoting single-chain conformational compactness and phase separation. We found further that $T_{cr}^* \propto -\text{SCD}$, where SCD is a recently proposed "sequence charge decoration" parameter that is determined solely by sequence information. Ramification of our findings for deciphering the sequence dependence of the phase separation of intrinsically disordered proteins are discussed.

Received for publication 1 Jan 0000 and in final form 1 Jan 0000.

Address reprint requests and inquiries to H. S. Chan, E-mail: chan@arrhenius.med.toronto.edu

The biological function and disease-causing malfunction of proteins are underpinned by their structures, dynamics, and myriad intra- and inter-molecular interactions. It is now clear that many critical cellular functions are carried out by intrinsically disordered proteins or protein regions (collectively abbreviated as IDPs below) with amino acid sequences that are less hydrophobic than those of globular proteins but are enriched in charged, polar, and aromatic residues (1–6). Indeed, at least 75% of IDPs are polyampholytes (7, 8) in that they contain both positively and negatively charged residues (9, 10). Accordingly, electrostatic effects are an important factor in determining individual IDPs' conformational dimensions (8, 11, 12) and binding (13, 14). Charge-charge interactions are often significant in the recently discovered phenomenon of functional IDP liquid-liquid phase separation as well (15–22). IDP phase separation appears to be the physical basis of membraneless organelles, performing many vital tasks. Recent examples include subcompartmentalization within the nucleolus (22) and synaptic plasticity (21). Malfunction of phase separation processes can lead to disease-causing amyloidogenesis (18) and neurological disorders (21). Speculatively, membraneless liquid-liquid phase separation of biomolecules might even have played a role in the origins of life (23).

Electrostatic effects encoded by a sequence of charges on a chain molecule depend not only on the total positive and negative charges or net charge (24, 25) but also, and ultimately, on the charge pattern (8). In the IDP context, this was demonstrated clearly by Das and Pappu who conducted explicit-chain, implicit-solvent conformational sampling of thirty different sequences each composing of 25 lysine (K)

and 25 glutamic acid (E) residues (termed KE sequences hereafter). They found that the average radius of gyration, $\langle R_g \rangle$, is strongly sequence-dependent, and is correlated with a charge pattern parameter κ that quantifies local deviations from global charge asymmetry (8). A subsequent analytical treatment of the KE sequences by Sawle and Ghosh rationalized the trend through another charge pattern parameter "sequence charge decoration" (SCD) that also correlates well with $\langle R_g \rangle$ (26). For IDP phase separation, a recent sequence-dependent random-phase-approximation (RPA) approach we put forth (27, 28) accounted for the experimental difference in phase-separation tendency between the wildtype and a charge-scrambled mutant of the 236-residue N-terminal fragment of DEAD-box RNA helicase Ddx4 (16).

These advances suggest that a deeper understanding of the relationship between single- and multiple-chain IDP properties is in order, and that such a fundamental relationship is worth pursuing for theoretical as well as practical reasons. It would be very helpful, for instance, if experimental measurements on single-chain properties can infer the conditions under which a protein sequence would undergo multiple-chain phase separation. Here we embark on this endeavor by first focusing on electrostatic interactions, while leaving the study of aromatic and other π -interactions—which can also figure prominently in IDP behavior (16, 27, 29)—to future effort. To reach this initial goal, we apply our RPA formulation to the aforementioned thirty KE sequences of length $N = 50$ to ascertain their phase-separation properties under salt-free conditions. Adopting our previous notation and making the same simplifying assumption that amino acid residues and water molecules are of equal size in the theory (27, 28), the

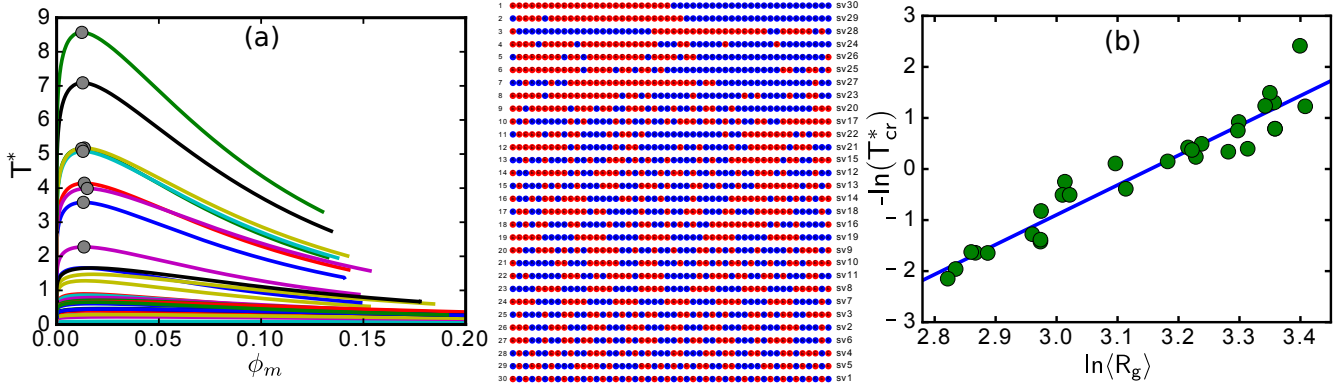


FIGURE 1 Phase behavior and conformational compactness of the thirty KE sequences studied. (a) Coexistence curves in different colors are for the sequences 1–30 (right, K and E residues are shown in red and blue respectively) listed in descending order of T_{cr}^* . Critical points ($T^* = T_{cr}^*$) for several high- T_{cr}^* sequences are marked (grey circles). The “sv” sequence labels are those in (8). (b) Logarithmic correlation between RPA-predicted T_{cr}^* and $\langle R_g \rangle$ simulated in (8) (green circles). The best-fitted line shown is $-\ln T_{cr}^* = -18.4 + 5.83 \ln\langle R_g \rangle$ with squared Pearson coefficient $r^2 = 0.92$.

free energy F_{RPA} of the multiple-chain system of a given polyampholytic sequence with charge pattern $\{\sigma_i\} = \{\sigma_1, \sigma_2, \dots, \sigma_N\}$, where $\sigma_i = \pm 1$ is the sign of electronic charge of the i th residue, is given by [see Eqs. (13) and (40) of Ref. (28)]:

$$\frac{F_{RPA} a^3}{V k_B T} = \frac{\phi_m}{N} \ln \phi_m + (1 - \phi_m) \ln(1 - \phi_m) + \int_0^\infty \frac{dk k^2}{4\pi^2} \{ \ln[1 + \mathcal{G}(k)] - \mathcal{G}(k) \}, \quad (1)$$

where $a = 3.8 \text{ \AA}$ is the $C\alpha$ - $C\alpha$ distance, V is system volume, k_B is Boltzmann constant, T is absolute temperature, and $\phi_m = \rho_m a^3$ is the volume ratio of amino residues wherein ρ_m/N is protein density. Moreover,

$$\mathcal{G}(k) = \frac{4\pi\phi_m}{k^2(1 + k^2)T^*N} \langle \sigma | \hat{G}_M(k) | \sigma \rangle, \quad (2)$$

where $|\sigma\rangle$ and $\langle\sigma|$ ($\equiv |\sigma\rangle^T$) are the N -dimensional column and row vectors, respectively, for the sequence charge pattern, i.e., $|\sigma\rangle_i = \sigma_i$, and the symmetric $N \times N$ matrix $\hat{G}_M(k)$ has elements $\hat{G}_M(k)_{ij} = \exp(-k^2|i - j|/6)$. The reduced temperature $T^* \equiv a/l_B$; $l_B = e^2/(4\pi\epsilon_0\epsilon_r k_B T)$ is the Bjerrum length, ϵ_0 is vacuum permittivity and ϵ_r is relative permittivity (27, 28). Here ϵ_r is treated as an unspecified constant because our focus is on the relative T_{cr}^* s of different sequences. It may be noted nonetheless that $\epsilon_r \approx 80$ for water but can be significantly lower for water-IDP solutions (28).

We determined the phase diagrams of the 30 KE sequences from the free energy expression Eq. (1) using standard procedures described in Ref. (28). For each sequence, the highest temperature on the coexistence curve is the critical temperature T_{cr}^* , which is the highest T^* at which phase separation can occur (Fig. 1(a)). The critical temperatures of the KE sequences exhibit significant diversity, ranging from

$T_{cr}^* = 0.089$ (sv1) to 8.570 (sv30). The variation of critical volume fraction $\phi_{cr} \equiv \phi_m(T_{cr}^*)$ from 0.0123 (sv30, sv24) to 0.0398 (sv1) is narrower. The KE sequences were originally labeled as sv1, sv2, ..., sv30 in ascending values for Das and Pappu's charge pattern parameter κ , from the strictly alternating sequence sv1 with $\kappa = 0.0009$ (minimum segregation of opposite charges) to the diblock sequence sv30 with $\kappa = 1.0$ (maximum charge segregation) (8). Our RPA-predicted T_{cr}^* s follow largely, though not exactly, the same order: sv1 and sv30 have the lowest and highest T_{cr}^* s, respectively; but, e.g., sv24 rather than sv27 has the fourth largest T_{cr}^* and sv5, not sv2, has the second lowest T_{cr}^* .

Because $\langle R_g \rangle$ correlates positively with κ (8), the present T_{cr}^* trend suggests that multiple-chain T_{cr}^* should correlate with single-chain $\langle R_g \rangle$. Indeed, a striking correlation (Fig. 1(b)) satisfying the approximate power-law

$$T_{cr}^* \approx 9.8 \times 10^7 \langle R_g \rangle^{-5.83}, \quad (3)$$

with R_g in units of \AA , is observed for the KE sequences. The positive (T_{cr}^*) - $\langle R_g \rangle$ correlation may be understood qualitatively by considering two extreme cases: The diblock and the strictly alternating sequences (Fig. 2). For the diblock, attractive interactions are absent—cannot be satisfied—within most stretches of several (e.g. < 6) residues. However, once a pair of opposite charges are in spatial proximity, chain connectivity brings two oppositely charged blocks together, leading to a strong Coulomb attraction, thus a small $\langle R_g \rangle$ and a higher tendency to phase separate (higher T_{cr}^*). In contrast, for the strictly alternating sequence, attractive Coulombic interactions that are already weakened relative to that of the diblock sequence require more conformational restriction, resulting in more open, large- $\langle R_g \rangle$ single-chain conformations and less tendency to phase separate (lower T_{cr}^*).

At this juncture, it is instructive to compare the predictive power of κ and another charge pattern parameter $SCD \equiv \sum_{i < j}^N \sigma_i \sigma_j \sqrt{j - i} / N$ that has emerged from the analysis

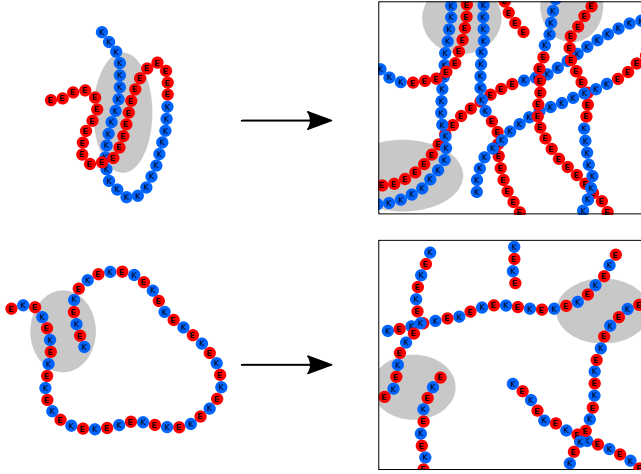


FIGURE 2 Schematics: similar electrostatic effects are at play in single-chain compactness (left) and multiple-chain phase separation (right). Top: Long stretches of like charges entails strong intra- and interchain attractions (grey areas). Favorable intrachain interactions are among residues nonlocal, i.e., more than a few residues apart, along the chain sequence. Most local interactions are repulsive because of the charge blocks. Bottom: Attraction within and among polyampholytes that lack long charge blocks are weaker. Overall attractive interactions now require conformationally restrictive charge pairings and are weaker because of repulsion from neighboring like charges.

of Sawle and Ghosh (26). The two parameters are well correlated ($r^2 = 0.95$, see Fig. 7 of Ref. (26)), yet the variation of both T_{cr}^* and $\langle R_g \rangle$ of the KE sequences is significantly smoother with respect to SCD than κ (Fig. 3). For example, despite the large variation in κ for sv24, sv26, and sv28 (0.4456, 0.6102, and 0.7666, respectively), their $\langle R_g \rangle = 17.6$, 17.5, and 17.9 Å (8), and their $T_{cr}^* = 5.160$, 5.080, and 5.177 are almost identical (Fig. 3(b)). This similarity, however, is well reflected by their similar SCD = -17.00, -16.21, and -15.99. Indeed, a near-linear relationship ($r^2 = 0.997$),

$$T_{cr}^* \approx -0.314(\text{SCD}) , \quad (4)$$

is observed (Fig. 3(b)). A likely origin of SCD's better performance is that it accounts for potential interactions between charges far apart along the chain sequence whereas κ relies on averaging over 5 or 6 consecutive charges. For the same reason, SCD is less sensitive than κ to isolated charge reversals. Future effort should be directed toward further assessment of these and other possible charge pattern parameters (31) as predictors for IDP conformational properties.

In summary, we have quantified a close relationship between single-chain conformational compactness of polyampholytes and their phase separation tendency. The above RPA results were derived with a short-range cutoff for Coulomb interactions to account for residue sizes (28, 30). If we had adopted an unphysical interaction scheme without such a cutoff, similar trends would still be observed although the scaling relations Eqs. (3) and (4) would be modified, respectively, to $T_{cr}^* \sim (R_g)^{-3.57}$ and $T_{cr}^* \approx -0.490(\text{SCD})$. Thus,

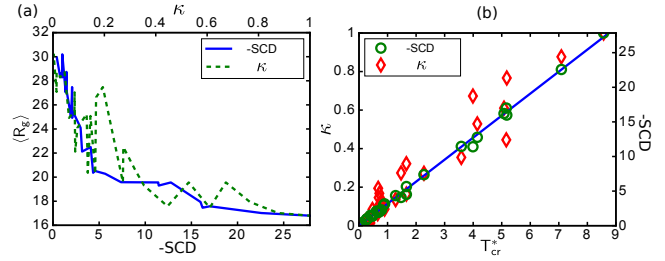


FIGURE 3 Charge-pattern parameters. (a) Single-chain $\langle R_g \rangle$ in (8) versus the κ parameter of Das and Pappu (8) (top horizontal scale) and the SCD parameter of Sawle and Ghosh (26) (bottom scale for -SCD). (b) Variation of RPA-predicted T_{cr}^* with κ (left vertical scale) and -SCD (right vertical scale).

in any event, basic physics dictates a positive correlation between T_{cr}^* and $\langle R_g \rangle$. This connection should be further explored by both theory and simulation (31, 32) to help decipher the sequence determinants of IDP phase separation.

AUTHOR CONTRIBUTIONS

Y.-H.L. and H.S.C. designed research, performed research, analyzed data. and wrote the article.

ACKNOWLEDGMENTS

We thank Julie Forman-Kay and Robert Vernon for helpful discussions. This work was supported by Canadian Cancer Society Research Institute grant no. 703477, Canadian Institutes of Health Research grant MOP-84281, and computational resources provided by SciNet of Compute Canada.

REFERENCES and FOOTNOTES

1. Uversky, V. N., J. R. Gillespie, and A. L. Fink. 2000. Why are natively unfolded proteins unstructured under physiologic conditions? *Proteins* 41:415–427.
2. Tompa, P. 2012. Intrinsically unstructured proteins: a 10-year recap. *Trends Biochem. Sci.* 37:509–516.
3. Forman-Kay, J. D. and T. Mittag. 2013. From sequence and forces to structure, function, and evolution of intrinsically disordered proteins *Structure* 21:1492–1499.
4. van der Lee, R., M. Buljan, B. Lang, R. J. Weatheritt, G. W. Daughdrill, A. K. Dunker, M. Fuxreiter, J. Gough, J. Gsponer, D. T. Jones, P. M. Kim, R. W. Kriwacki, C. J. Oldfield, R. V. Pappu, P. Tompa, V. N. Uversky, P. E. Wright, and M. M. Babu. 2014. Classification of intrinsically disordered regions and proteins. *Chem. Rev.* 114:6589–6631.
5. Chen, T., J. Song, and H. S. Chan. 2015. Theoretical perspectives on nonnative interactions and intrinsic disorder in protein folding and binding. *Curr. Opin. Struct. Biol.* 30:32–42.

REFERENCES AND FOOTNOTES

6. Das, R. K., K. M. Ruff, and R. V. Pappu. 2015. Relating sequence encoded information to form and function of intrinsically disordered proteins. *Curr. Opin. Struct. Biol.* 32:102–112.
7. Sickmeier, M., J. A. Hamilton, T. LeGall, V. Vacic, M. S. Cortese, A. Tantos, B. Szabo, P. Tompa, J. Chen, V. N. Uversky, Z. Obradovic, and A. K. Dunker. 2007. DisProt: the database of disordered proteins. *Nucl. Acids Res.* 35:D786–D793.
8. Das, R. K. and R. V. Pappu. 2013. Conformations of intrinsically disordered proteins are influenced by linear sequence distributions of oppositely charged residues. *Proc. Natl. Acad. Sci. USA* 110:13392–13397.
9. Higgs, P. G. and J. -F. Joanny. 1991. Theory of polyampholyte solutions. *J. Chem. Phys.* 94:1543–1554.
10. Dobrynin, A. V., R. H. Colby, and M. Rubinstein. 2007. Polyampholytes. *J. Polym. Sci. Part B Polym. Phys.* 42:3513–3538.
11. Liu, B., D. Chia, V. Csizmok, P. Farber, J. D. Forman-Kay, and C. C. Gradinaru. 2014. The effect of intrachain electrostatic repulsion on conformational disorder and dynamics of the Sic1 protein. *J. Phys. Chem. B* 118:4088–4097.
12. Song, J., G. N. Gomes, C. C. Gradinaru, and H. S. Chan. 2015. An adequate account of excluded volume is necessary to infer compactness and asphericity of disordered proteins by Förster resonance energy transfer. *J. Phys. Chem. B* 119:15191–15202.
13. Borg, M., T. Mittag, T. Pawson, M. Tyers, J. D. Forman-Kay, and H. S. Chan. 2007. Polyelectrostatic interactions of disordered ligands suggest a physical basis for ultrasensitivity. *Proc. Natl. Acad. Sci. USA* 104:9650–9655.
14. Csizmok, V., S. Orlikcym J. Cheng, J. Song, A. Bah, N. Delgosaie, H. Lin, T. Mittag, F. Sicheri, H. S. Chan, M. Tyers, and J. D. Forman-Kay. 2017. Al allosteric conduit facilitates dynamic multisite substrate recognition by the SCF^{Cdc4} ubiquitin ligase. *it Nat. Comm.* 8:13943.
15. Toretzky, J. A. and P. E. Wright. 2014. Assemblages: Functional units formed by cellular phase separation. *J. Cell. Biol.* 206:579–588.
16. Nott, T. J., E. Petsalaki, P. Farber, D. Jervis, E. Fussner, A. Plochowietz, T. D. Craggs, D. P. Bazett-Jones, T. Pawson, J. D. Forman-Kay, and A. J. Baldwin. 2015. Phase transition of a disordered nuage protein generates environmentally responsive membraneless organelles. *Mol. Cell* 57:936–947.
17. Brangwynne, C. P., P. Tompa, and R. V. Pappu. 2015. Polymer physics of intracellular phase transitions *Nat. Phys.* 11:899–904.
18. Molliex, A., J. Temirov, J. Lee, M. Coughlin, A. P. Kanagaraj, H. J. Kim, T. Mittag, and J. P. Taylor. 2015. Phase separation by low complexity domains promotes stress granule assembly and drives pathological fibrillization. *Cell* 163:123–133.
19. Bergeron-Sandoval, L.-P., N. Safaee, and S. W. Michnick. 2016. Mechanisms and consequences of macromolecular phase separation. *Cell* 165:1067–1079.
20. Pak, C. W., M. Kosno, A. S. Holehouse, S. B. Padrick, A. Mittal, R. Ali, A. A. Yunus, D. R. Liu, R. V. Pappu, and M. K. Rosen. 2016. Sequence determinants of intracellular phase separation by complex coacervation of a disordered protein. *Mol. Cell* 63:72–85.
21. Zeng, M., Y. Shang, Y. Araki, T. Guo, R. L. Huganir, and M. Zhang. 2016. Phase transition in postsynaptic densities underlies formation of synaptic complexes and synaptic plasticity. *Cell* 166:1163–1175.
22. Feric, M., N. Vaidya, T. S. Harmon, D. M. Mitrea, L. Zhu, T. M. Richardson, R. W. Kriwacki, R. V. Pappu, and C. P. Brangwynne. 2016. Coexisting liquid phases underlie nucleolar subcompartments. *Cell* 165:1686–1697.
23. Keating, C. D. 2012. Aqueous phase separation as a possible route to compartmentalization of biological molecules. *Acc. Chem. Res.* 45:2114–2124.
24. Mao, A. H., S. L. Crick, A. Vitalis, C. L. Chicoine, and R. V. Pappu. 2010. Net charge per residue modulates conformational ensembles of intrinsically disordered proteins. *Proc. Natl. Acad. Sci. USA* 107:8183–8188.
25. Müller-Spätth, S., A. Soranno, V. Hirschfeld, H. Hofmann, S. Rügger, L. Reymond, D. Nettels, and B. Schuler. 2010. Charge interactions can dominate the dimensions of intrinsically disordered proteins. *Proc. Natl. Acad. Sci. USA* 107:14609–14614.
26. Sawle, L. and K. Ghosh. 2015. A theoretical method to compute sequence dependent configurational properties in charged polymers and proteins. *J. Chem. Phys.* 143:085101.
27. Lin, Y.-H., J. D. Forman-Kay, and H. S. Chan. 2016. Sequence-specific polyampholyte phase separation in membraneless organelles. *Phys. Rev. Lett.* 117:178101.
28. Lin, Y.-H., J. Song, J. D. Forman-Kay, and H. S. Chan. 2017. Random-phase-approximation theory for sequence-dependent, biologically functional liquid-liquid phase separation of intrinsically disordered proteins. *J. Mol. Liq.* 228:176–193.
29. Song, J., S. C. Ng, P. Tompa, K. A. W. Lee, and H. S. Chan. 2013. Polycation- π interactions are a driving force for molecular recognition by an intrinsically disordered oncoprotein family. *PLoS Comput. Biol.* 9:e1003239.
30. Ermoshkin, A. V. and M. Olvera de la Cruz. 2003. Polyelectrolytes in the presence of multivalent ions: gelation versus segregation. *Phys. Rev. Lett.* 90:125504.
31. Holehouse, A. S., R. K. Das, J. N. Ahad, M. O. G. Richardson, and R. V. Pappu. 2017. CIDER: Resources to analyze sequence-ensemble relationships of intrinsically disordered proteins. *Biophys. J.* 112:16–21.

REFERENCES AND FOOTNOTES

REFERENCES AND FOOTNOTES

32. Ruff, K. M., T. S. Harmon, and R. V. Pappu. 2015. CAMELOT: A machine learning approach for coarse-grained simulations of aggregation of block-copolymeric protein sequences. *J. Chem. Phys.* 143:243123.